CONTACT INSTABILITY IN RATE-CONTROL TELEMANIPULATION

Chi-Cheng Cheng and Jiun-Hung Chen

Department of Mechanical and Electro-Mechanical Engineering,
National Sun Yat-Sen University, 70 Lian-Hai Road, Kaohsiung
Taiwan 80424, Republic of China

Abstract: Telemanipulation is usually provided with the force-reflective feature to give human operators information about the remote site. However, oscillations can always been found in contact with rigid environment. This paper presents theoretical analysis about the phenomenon of the contact oscillation in rate-control manipulation using the describing function technique. Occurrence and characteristics of limit cycles due to contact motion are verified by results of computer simulations.

Keywords: Limit cycles, Oscillation, Robot dynamics, Telemanipulation, Teleoperation, Telerobotics.

1. INTRODUCTION

The master-slave manipulator was introduced about a half century ago. This special robotic framework comprises of a master manipulator and a slave manipulator. The master side is operated by a human operator and the slave one follows the commands exerted at the master to execute designated missions. Since the master-slave manipulator is able to transfer dexterous skills of human operators to the distant or hazardous environment, it has been widely applied in undersea, space, radioactive fields, and medical operations, etc. In those applications, the master-slave manipulator borrows high adaptability and robustness from the human to perform tasks in unknown and time-varying environment.

The master-slave manipulator actually functions as an interface between the human operator and the environment. Therefore, this interface should be transparent enough so that the operator seems to directly perform tasks at the working site to reduce possible manipulation deviations. The first electrically controlled master-slave manipulator was developed in 1950s (Goertz and Thompson, 1954). This milestone work produced control signal based on the position difference between both manipulators. In order to give the human operator ability to feel the contact force on the slave side, a force-reflective technique was also presented. This achievement initiated the concept of telepresence (Sheridan, 1989). Furthermore, performance evaluation of a six-axis force reflecting telemanipulator conducted by Hannaford *et al*. (1991) demonstrated that manipulation fulfillment was benefited by the feature of force reflection.

Robots in force control mode often become unstable during contact with stiff environment. The problem of contact oscillations in a force-controlled robot has long been recognized and studied. Based on the stability analysis in discrete-time domain, Whitney (1985) indicated that at a fixed sampling rate there was a stability trade-off between the force feedback gain and the stiffness of the environment. This conclusion has been substantiated via study of bandwidth limitations in robot force control by Eppinger and Seering (1987). Kazerooni (1990) also raised a sufficient condition for the stability of robot manipulators in constrained maneuvers. Besides, in order to deeply understand the contact instability, the oscillatory behavior in contact motion of robots was examined via both the simulation and the experiment approaches (Ferretti *et al*., 1991; Ferretti *et al*., 1999).

Similar contact stability problem exists in the teleoperator system because of interaction between the slave manipulator and the environment. Through

experimental and simulation studies of a single-degree-of-freedom teleoperator system, Hannaford and Anderson (1988) showed that human operator properties affected the stability of the system in hard contact tasks. A strong grip on the master side increases the local damping feedback to the hand controller, which in turn, improves the stability of the system. Furthermore, position control and rate control are two common manual control modes in teleoperation. Kim *et al*. (1987) evaluated human operator performance using these two modes through simulated three-axis pick-and-place tasks. Experimental results indicated that position control was recommended for small-work-space telemanipulation tasks, while rate control was suitable for slow wide-work-space operations. Chin (1991) verified that oval-shape limit cycles with negative offset appeared for zero-damping position-control telemanipulation using the approach of energy conservation.

2. DESCRIBING FUNCTION METHOD

The describing function method has been a standard and efficient way to estimate characteristics of possible limit cycles in nonlinear systems. A nonlinear plant can be treated as a linear transfer function by approximating its sinusoidal response with the fundamental harmonic, under the assumption of low-pass property in the system. Therefore, analysis techniques for linear systems can be easily applied. The null-offset describing function method is almost found in every textbook in the fields of analysis of nonlinear systems or nonlinear control systems. A generalized describing function approach adopted from (Khalil, 1992) is summarized here for the purpose of self-contained exposition.

Consider an autonomous nonlinear system, which consists of a linear time-invariant plant $G(s)$ and a memoryless time-invariant nonlinear function ψ, as shown in Fig. 1. Assume the output $y(t)$ is a steady periodic function with a period of $2\pi/\omega$ under the condition of a constant input r. Then both the output of the nonlinear function $\psi(t)$ and $y(t)$ can be formulated in terms of Fourier series, i.e.,

$$\psi(y) = \sum_{k=-\infty}^{\infty} c_k \exp(jk\omega t), \text{ and} \tag{1}$$

$$y(t) = \sum_{k=-\infty}^{\infty} a_k \exp(jk\omega t), \tag{2}$$

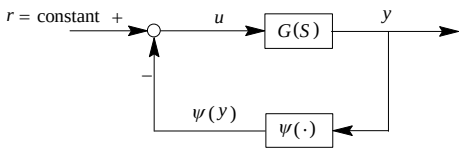

Fig. 1. A control system with a nonlinear function feedback.

where

$$a_k = \overline{a}_{-k} \text{ and}$$

$$c_k = \overline{c}_{-k} = \frac{1}{2\pi}\int_0^{2\pi} \psi(y)\exp(-jk\omega t)d(\omega t). \tag{3}$$

Incorporating the above expressions,

$$G(jk\omega) = \overline{G}(-jk\omega), \tag{4}$$

and the low-pass characteristics of $G(s)$ into the closed-loop relationship

$$y(t) = [r - \psi(y)]G(P), \tag{5}$$

where P denotes the derivative operator, i.e., d/dt, leads to the following equations:

$$\begin{cases} G(0)c_0 + a_0 = G(0)r \\ G(j\omega)c_1 + a_1 = 0, \end{cases} \tag{6}$$

Let the limit cycle at $y(t)$ have the form of

$$y(t) = a_0 + a\sin\omega t, \tag{7}$$

where a_0 and a are the offset and the amplitude of the limit cycle, respectively. It can be easily concluded that

$$a_1 = \frac{a}{2j}. \tag{8}$$

Therefore, (6) can be reduced to

$$a_0 G(0)N_0 + a_0 = G(0)r \tag{9}$$

$$G(j\omega)N_1 + 1 = 0, \tag{10}$$

where N_0 and N_1 actually indicate coefficients of the describing function of the nonlinear function ψ, and are defined by

$$N_0 = \frac{c_0(a_0, a)}{a_0} \text{ and } N_1 = j\frac{2c_1(a_0, a)}{a}. \tag{11}$$

As a result, three unknowns, a_0, a, and ω for possible limit cycles can be resolved. Cook (1994) summarized that a necessary condition for a stable limit cycle is

$$0 < \angle\eta - \angle\xi < \pi, \tag{12}$$

where

$$\xi = \frac{\partial G(j\omega)}{\partial\omega} \text{ and } \eta = \frac{\partial}{\partial a}\left(\frac{-1}{N_1(a)}\right). \tag{13}$$

3. ENVIRONMENT DESCRIPTION

The master-slave manipulator locates between the human operator and the environment. In order to allow the dexterity of human operators can be fully transferred to the working site, this interface needs be as transparent as possible. Under the assumption of ideal transparency, the dynamic equation for the human interacting with the environment via the tele-manipulator can be established as

$$J_h\ddot{\theta}_s + B_h\dot{\theta}_s + K_h\theta_s = \tau_h - \tau\,, \tag{14}$$

where J_h, B_h, and K_h respectively denote the effective moment of inertia, viscous damping coefficient, and stiffness of the human operator. The active part τ_h is generated by human's muscles and should be dependent on states of muscles. τ represents the reaction torque due to the contact with the environment.

When the slave touches an obstacle in the environment, an interaction force appears at the contact surface. Assume that the environment is modeled as a linear spring with a spring constant K_{en} as illustrated in Fig. 2. Then the relationship between the slave manipulator and the environment can be described as a piecewise linear function shown in Fig. 3. Hence the contact force becomes

$$\begin{cases} 0 & ,\theta_s < \theta_{en} \\ K_{en}(\theta_s - \theta_{en}) & ,\theta_s \ge \theta_{en} \end{cases}, \tag{15}$$

where θ_s and θ_{en} represent the displacement of the slave manipulator and the position where the obstacle locates, respectively. Without loss of generality, θ_{en} is assumed to be zero for simplification of equation derivation hereinafter.

Let the input to the nonlinear function be $a_0 + a\sin\omega t$, where a is a positive number. Apparently, the plant will degenerate to a simple linear spring for $a_0 \ge a$ and a null function for $a_0 < -a$, respectively. Therefore, its corresponding describing function only needs to be discussed in the situation of $a > |a_0|$. After a number of mathematical manipulations based on (3), the coefficients of the describing function can be obtained as follows:

$$c_0 = K_{en}\left[\frac{a_0}{2} + \frac{a_0}{\pi}\sin^{-1}\left(\frac{a_0}{a}\right) + \frac{a}{\pi}\sqrt{1-\left(\frac{a_0}{a}\right)^2}\right] \tag{16}$$

$$c_1 = -\frac{jK_{en}}{2}\left[\frac{a}{2} + \frac{a}{\pi}\sin^{-1}\left(\frac{a_0}{a}\right) + \frac{a_0}{\pi}\sqrt{1-\left(\frac{a_0}{a}\right)^2}\right] \tag{17}$$

4. ANALYSIS OF CONTACT BEHAVIOR

An ideal tele-manipulator interacting with its environment can be modeled as a control system shown in Fig. 1. In the block diagram, the nonlinear function ψ is defined in Fig. 3. To simplify the following mathematical derivation, assumptions of $\theta_{en} = 0$ and $\tau_h = 0$ are made.

To investigate the occurrence of contact oscillation when the slave manipulator touches the environment is equivalent to analyze if the control system described in Fig. 1 owns limit cycles. In other words, it needs to explore if (9) and (10) have non-trivial solutions for (a_0, a, ω), where c_0 and c_1 are formulated as (16) and (17). N_0 and N_1 can be rewritten by incorporating (16) and (17) into (11).

$$N_0 = K_{en}\left[\frac{1}{2} + \frac{1}{\pi}\sin^{-1}\left(\frac{a_0}{a}\right) + \frac{a}{\pi a_0}\sqrt{1-\left(\frac{a_0}{a}\right)^2}\right] \tag{18}$$

$$N_1 = K_{en}\left[\frac{1}{2} + \frac{1}{\pi}\sin^{-1}\left(\frac{a_0}{a}\right) + \frac{a_0}{\pi a}\sqrt{1-\left(\frac{a_0}{a}\right)^2}\right] \tag{19}$$

Since $a > |a_0| \ge 0$, the constraint inequalities for the offset-amplitude ratio a_0/a can be solved as follows:

$$-1 < \frac{a_0}{a} < 1 \quad \text{and} \quad a > 0 \tag{20}$$

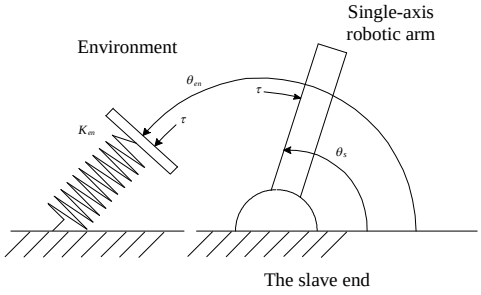

Fig. 2. A single-link manipulator and an environment modeled as a linear spring.

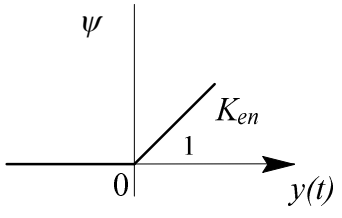

Fig. 3. The relationship between the displacement of the manipulator and the induced torque from the environment.

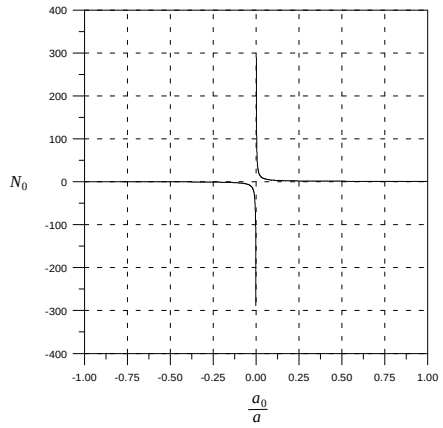

Fig. 4. The relationship between N_0 and the offset-amplitude ratio a_0/a.

The plot of N_0 versus a_0/a is illustrated in Fig. 4. Once the value of a_0/a is determined, $-1/N_1$ can also be calculated from (19) as a point on the real axis. Whether there exists a limit cycle depends on if there is any intersection between the Nyquist plot of $G(j\omega)$ and $-1/N_1$.

A common type of manipulation is categorized as the rate-control mode, which employs the displacement of the master as the velocity command for the slave end. In this case, there becomes zero stiffness between the input torque and the angular displacement output. In other words, there will be a pole at the origin in the transfer function.

Given the transfer function below

$$G(s) = \frac{k}{s(J_h s^2 + B_h s + K_h)} \tag{21}$$

$G(0)$ appears to be infinite. Therefore, (6) reduces to

$$\begin{cases} c_0 = r \\ G(j\omega)N_1 + 1 = 0, \end{cases} \tag{22}$$

Consequently, the following equations can be obtained.

$$\begin{cases} a_0 N_0 = r \\ G(j\omega) = -\dfrac{1}{N_1} \end{cases} \tag{23}$$

where N_0 and N_1 are determined in (18) and (19).

Since a_0/a locates between -1 and 1, the value of $-1/N_1$ is in the interval of $(-\infty, -1/K_{en})$. If these is an intersection between the trajectories of $-1/N_1$ and $G(j\omega)$ in the complex plane as shown in Fig. 5, the

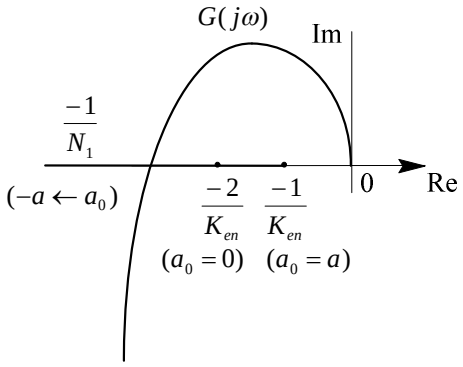

Fig. 5. Nyquist plot of $G(j\omega)$ for rate-control telemanipulation.

intersection point provides solutions of the frequency ω and the offset-amplitude ratio a_0/a for the limit cycle of contact oscillation. It can be easily obtained that the trajectory of $G(j\omega)$ crosses over the real axis at $-(kJ_h)/(B_h K_h)$ on the real axis when $\omega = (K_h/J_h)^{1/2}$, which is independent of the property of the environment. In other words, contact oscillation may occur with a fixed frequency if the following situation is satisfied.

$$\frac{kJ_h}{B_h K_h} > \frac{1}{K_{en}} \tag{24}$$

Furthermore, the sign of the offset a_0 can also be concluded according to the position of the intersection, i.e.,

$$a_0 > 0, \quad \text{if } \frac{2}{K_{en}} > \frac{kJ_h}{B_h K_h} > \frac{1}{K_{en}} \tag{25}$$

$$a_0 < 0, \quad \text{if } \frac{kJ_h}{B_h K_h} > \frac{2}{K_{en}} \tag{26}$$

Once a_0/a is determined, the offset a_0 has the following expression based on (23).

$$a_0 = \frac{r}{N_0(a_0/a)} \tag{27}$$

Because of the fact of $a > |a_0| \geq 0$, the value of a can therefore be obtained. A special case exists when $a_0/a = 0$. This condition indicates zero-offset oscillations. Consequently, the expression for the amplitude a becomes

$$a = \frac{\pi r}{K_{en}} \tag{28}$$

As a result, the behavior of the contact oscillation is fully resolved.

Characteristics of the contact oscillation caused by nonlinear limit cycle are summarized as follows:

1) Contact oscillation may occur if the trajectory of $G(j\omega)$ intersects $-1/N_1$ on the negative real axis, i.e.,

$$\frac{kJ_h}{B_h K_h} > \frac{1}{K_{en}} \tag{29}$$

2) The resulting limit cycle has a fixed offset-amplitude ratio a_0/a and a constant oscillatory frequency $(K_h/J_h)^{1/2}$ for a given input r. Besides, the relationships among a_0, a, and r can also be expressed by

$$a \propto r, \text{ and} \tag{30}$$
$$a_0 \propto r \text{ for } a_0 \neq 0. \tag{31}$$

3) When the stiffness of environment K_{en} approaches to zero, the right most point of the path of $-1/N_1$, $-1/K_{en}$, becomes negative infinite and it is highly impossible for the trajectory $G(j\omega)$ to intersect with $-1/N_1$. Therefore, no limit cycle occurs. If K_{en} increases, $-1/K_{en}$ tends to move toward the origin. Then the possibility for intersection grows and the system tends to bring about the contact oscillation.

5. SIMULATION STUDIES

Consider a rate-controlled manipulation with

$$G(s) = \frac{k}{s(s^2 + s + 1)}. \tag{32}$$

Given input r is illustrated in Fig. 6. Phenomenon of contact oscillations for different values of k under constant environmental stiffness $K_{en} = 1$ will be investigated.

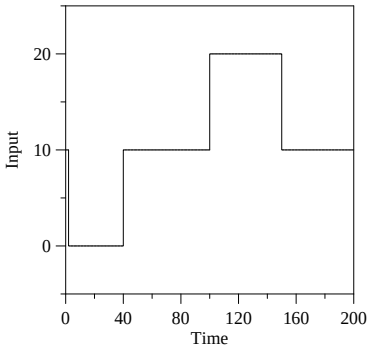

Fig. 6. The reference command input for an example rate-controlled manipulation.

The Nyquist plot of $G(j\omega)$ crosses the real axis at the point of $(-k,0)$ for $\omega = 1$. The relative position of this intersection point with respect to $-1/K_{en}$ or -1 determines whether the contact oscillation appears or not. Fig. 7 shows the dynamic behavior of the output of the system for different k.

If k is equal to 2.5, a limit cycle arises because of $-k$ less than -1 and is illustrated in Fig. 7(a). The offset of the limit cycle a_0 appears to be negative due to the fact of $-k < -2/K_{en}$. Besides, both the offset and amplitude of the limit cycle are multiplied by two when the input r doubles in the time interval (100, 150).

Fig. 7(b) depicts the output response when k is 2. Since $-k$ is equal to $-2/K_{en}$, the offset of the limit cycle becomes zero. When k is 1.5, the limit cycle has a positive offset as shown in Fig. 7(c) because of $-2/K_{en} < -k < -1/K_{en}$. But no limit cycle occurs if k is equal to 0.5. Because there is no intersection between $G(j\omega)$ and $-1/N_1$. This phenomenon is illustrated in Fig. 7(d). Different values of k demonstrated distinct behavior of nonlinear dynamics, which agrees with the results of the describing function analysis.

6. CONCLUSIONS

Contact oscillations for telemanipulators interacting with hard environment are caused by nonlinear limit cycles in the man-machine system. For rate-control telemanipulation, it is highly possible to bring about contact oscillations for environment with higher stiffness. If contact oscillation exists, greater and lower controller gains can always result in negative and positive offsets, respectively. Consider the condition with constant command. Both the amplitude and the offset of the limit cycle appear to be proportional to the magnitude of the command. However, the resulted limit cycle will always have a fixed offset-amplitude ratio and a constant oscillation frequency.

REFERENCES

Chin, K.P. (1991). *Stable Teleoperation with Optimal Performance*. Ph.D. Dissertation, Dept. Mech. Eng., Mass. Inst. Tech., Cambridge, MA, USA.

Cook, P.A. (1994). *Nonlinear Dynamical Systems*, 2nd Ed., Prentice-Hall, Englewood Cliffs, New Jersey.

Eppinger, S.D. and W. P. Seering (1987). Understanding bandwidth limitations in robot force control. In: *Proc. IEEE Int. Conf. Robotics and Automation*, pp. 904-909.

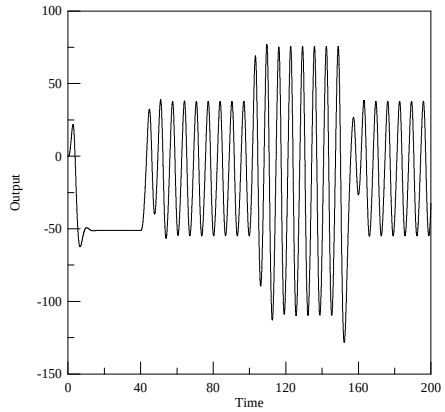

(a)

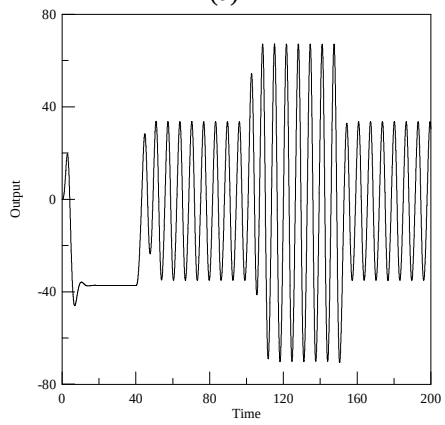

(b)

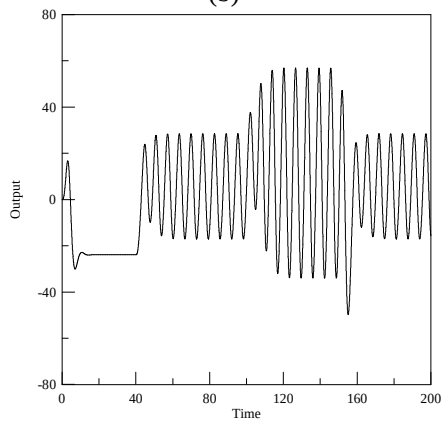

(c)

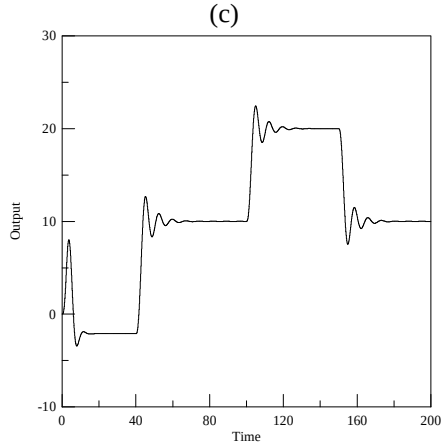

(d)

Fig. 7. Responses of the output for an example rate-controlled manipulation for different k values: (a) $k = 2.5$, (b) $k = 2$, (c) $k = 1.5$, and (d) $k = 0.5$.

Ferretti, G., C. Maffezzoni and G. Magnani (1991). Simulating rigid robots constrained by stiff contact. In: *Proc. 5th Int. Conf. Advanced Robotics*, pp. 1461-1464.

Ferretti, G., G. Magnani, and P. Rocco (1999). Force oscillations in contact motion of industrial robots: An experimental investigation. *IEEE Trans. Mechatronics*, **4**, 86-91.

Goertz, R.C. and W.M. Thompson (1954). Electronically controlled manipulator. *Nucleonics*, **12**, 46-47.

Hannaford, B. and R. Anderson (1988). Experimental and simulation studies of hard contact in forced reflecting teleoperation. In: *Proc. IEEE Int. Conf. Robotics and Automation*, pp. 584-589.

Hannaford, B., L. Wood, D. McAffee and H. Zak (1991). Performance evaluation of a six-axis generalized force-reflecting teleoperator. *IEEE Trans. Systems, Man, and Cybernetics*, **21**, 620-633.

Kazerooni, H. (1990). Contact instability of the direct drive robot when constrained by a rigid environment. *IEEE Trans. Robotics and Automation*, **35**, 710-714.

Khalil, J.K. (1992). *Nonlinear Systems*, pp. 351-355, Macmillan, New York.

Kim, W. S., F. Tendick, S. R. Ellis and L. W. Park (1987). A comparison of position and rate control for telemanipulations with consideration of manipulator system dynamics. *IEEE Journal of Robotics and Automation*, **RA-3**, 426-436.

Sheridan, T.B. (1989). Telerobotics. *Automatica*, **25**, 487-507.

Whitney, D.E. (1985). Historical perspective and state of the art in robot force control. In: *Proc. IEEE Int. Conf. Robotics and Automation*, pp. 262-268.